Since January 2020 Elsevier has created a COVID-19 resource centre with free information in English and Mandarin on the novel coronavirus COVID-19. The COVID-19 resource centre is hosted on Elsevier Connect, the company's public news and information website.

The Journal of Molecular Diagnostics, Vol. 23, No. 8, August 2021

the Journal of Molecular Diagnostics
jmdjournal.org

SARS-CoV-2 RNA Quantification Using Droplet Digital RT-PCR

Natalie N. Kinloch,*† Gordon Ritchie,‡§ Winnie Dong,† Kyle D. Cobarrubias,† Hanwei Sudderuddin,† Tanya Lawson,‡ Nancy Matic,‡§ Julio S.G. Montaner,†¶ Victor Leung,‡§¶ Marc G. Romney,‡§ Christopher F. Lowe,‡§ Chanson J. Brumme,†¶ and Zabrina L. Brumme*†

From the Faculty of Health Sciences, Simon Fraser University, Burnaby, British Columbia; British Columbia Centre for Excellence in HIV/AIDS,† Vancouver, British Columbia; Division of Medical Microbiology and Virology,‡ St Paul's Hospital, Vancouver, British Columbia; and the Departments of Pathology and Laboratory Medicine,§ and Medicine,¶ University of British Columbia, Vancouver, British Columbia, Canada*

Accepted for publication April 29, 2021.

Address correspondence to Zabrina L. Brumme, Ph.D., Faculty of Health Sciences, Simon Fraser University, 8888 University Dr., Burnaby, BC V5A 1S6, Canada; or Chanson J. Brumme, Ph.D., Faculty of Medicine, St. Paul's Hospital, University of British Columbia, 675-1081 Burrard St., Vancouver, BC V6Z 1Y6, Canada. E-mail: zbrumme@sfu.ca or cbrumme@bccfe.ca.

Quantitative viral load assays have transformed our understanding of viral diseases. They hold similar potential to advance COVID-19 control and prevention, but SARS-CoV-2 viral load tests are not yet widely available. SARS-CoV-2 molecular diagnostic tests, which typically employ real-time RT-PCR, yield semiquantitative results only. Droplet digital RT-PCR (RT-ddPCR) offers an attractive platform for SARS-CoV-2 RNA quantification. Eight primer/probe sets originally developed for real-time RT-PCR–based SARS-CoV-2 diagnostic tests were evaluated for use in RT-ddPCR; three were identified as the most efficient, precise, and sensitive for RT-ddPCR–based SARS-CoV-2 RNA quantification. For example, the analytical efficiency for the E-Sarbeco primer/probe set was approximately 83%, whereas assay precision, measured as the coefficient of variation, was approximately 2% at 1000 input copies/reaction. Lower limits of quantification and detection for this primer/probe set were 18.6 and 4.4 input SARS-CoV-2 RNA copies/reaction, respectively. SARS-CoV-2 RNA viral loads in a convenience panel of 48 COVID-19–positive diagnostic specimens spanned a 6.2$\log_{10}$ range, confirming substantial viral load variation *in vivo*. RT-ddPCR–derived SARS-CoV-2 *E* gene copy numbers were further calibrated against cycle threshold values from a commercial real-time RT-PCR diagnostic platform. This log-linear relationship can be used to mathematically derive SARS-CoV-2 RNA copy numbers from cycle threshold values, allowing the wealth of available diagnostic test data to be harnessed to address foundational questions in SARS-CoV-2 biology. *(J Mol Diagn 2021, 23: 907–919; https://doi.org/10.1016/j.jmoldx.2021.04.014)*

Quantitative viral load assays have revolutionized our ability to manage viral diseases.[1–6] Although not yet widely available for SARS-CoV-2, quantitative assays could advance our understanding of COVID-19 biology and inform infection prevention and control measures.[7,8] Most SARS-CoV-2 molecular diagnostic assays, however, which use real-time RT-PCR to detect one or more SARS-CoV-2 genomic targets using sequence-specific primers coupled with a fluorescent probe, are only semiquantitative. These tests produce cycle threshold (C_t) values as readouts, which represent the PCR cycle where the sample began to produce fluorescent signal above background. Although each C_t value decrement corresponds to a roughly twofold higher viral load (due to the exponential nature of PCR amplification), C_t values cannot be directly interpreted as SARS-CoV-2 viral loads without calibration to a quantitative standard.[9,10] Rather, C_t values are interpreted as positive, indeterminate, or negative based on assay-specific cutoffs and evolving clinical guidelines. Due to differences in nucleic acid extraction method, viral target, and other parameters, C_t values are also not directly comparable across assays or technology platforms.

Funded by GenomeBC COVID-19 rapid response grant COVID-115 (Z.L.B. and C.F.L.), CIHR project grant PJT-159625 (Z.L.B.), and Public Health Agency of Canada COVID-19 Immunology Task Force COVID-19 Hot Spots Competition grant PHAC CA# 2021-HQ-000120 (Z.L.B. and M.G.R.). N.N.K. is supported by a Vanier Canada Graduate Scholarship. Z.L.B. holds a Scholar Award from the Michael Smith Foundation for Health Research.

C.J.B. and Z.L.B. contributed equally to this work as senior authors.

https://doi.org/10.1016/j.jmoldx.2021.04.014

Droplet digital RT-PCR (RT-ddPCR) offers an attractive platform for SARS-CoV-2 RNA quantification.[11,12] Like real-time RT-PCR, ddPCR employs target-specific primers coupled with a fluorescent probe, making it relatively straightforward to adapt assays. In ddPCR, however, each reaction is fractionated into 20,000 nL–sized droplets prior to massively parallel PCR amplification. At end point, each droplet is categorized as positive (target present) or negative (target absent), allowing for absolute target quantification using Poisson statistics. This sensitive and versatile technology has been used for mutation detection and copy number determination in the human genome,[13] target verification following genome editing,[14] and copy number quantification for viral pathogens.[15–21] Several real-time RT-PCR SARS-CoV-2—specific primer/probe sets have been used in RT-ddPCR ([11,12,22,23] and manufacturer's protocol) with results achieving high sensitivity in some reports,[12,22,24–26] but few studies have rigorously evaluated SARS-CoV-2–specific primer/probe set performance in RT-ddPCR using RNA as a template. Furthermore, no studies to our knowledge have calibrated SARS-CoV-2 viral loads to diagnostic test C_t values. Here, eight SARS-CoV-2–specific primer/probe sets, originally developed for real-time RT-PCR,[27] are evaluated for use in RT-ddPCR. The authors also derive a linear equation relating RT-ddPCR–derived SARS-CoV-2 viral loads and real-time RT-PCR–derived C_t values for a commercial diagnostic assay, the LightMix Modular SARS-CoV (COVID19) E-gene assay, allowing conversion of existing COVID-19 diagnostic results to viral loads.

Materials and Methods

Ethical Approval

This study was approved by the Providence Health Care/University of British Columbia and Simon Fraser University Research Ethics Boards under protocol H20-01055.

Table 1 SARS-CoV-2 Primer/Probe Sets Assessed for Use in RT-ddPCR

Source	Name	Gene target	Primer/probe	Sequence	Coordinates
Charité- Berlin	E-Sarbeco	*E*	Forward	5′-ACAGGTACGTTAATAGTTAATAGCGT-3′	26,269–26,294
			Reverse	5′-ATATTGCAGCAGTACGCACACA-3′	26,381–26,360
			Probe	5′-FAM-ACACTAGCC/ZEN/ATCCTTA CTGCGCTTCG-3IABkFQ-3′	26,332–26,357
Pasteur Institute	IP2	*ORF1a*	Forward	5′-ATGAGCTTAGTCCTGTTG-3′	12,690–12,707
			Reverse	5′-CTCCCTTTGTTGTGTTGT-3′	12,797–12,780
			Probe	5′-HEX-AGATGTCTT/ZEN/GTGCTG CCGGTA-3IABkFQ-3′	12,717–12,737
	IP4	*ORF1b*	Forward	5′-GGTAACTGGTATGATTTCG-3′	14,080–14,098
			Reverse	5′-CTGGTCAAGGTTAATATAGG-3′	14,105–14,123
			Probe	5′-FAM-TCATACAAA/ZEN/CCAC GCCAGG-3IABkFQ-3′	14,186–14,167
China CDC	China-ORF	*ORF1a*	Forward	5′-CCCTGTGGGTTTTACACTTAA-3′	13,342–13,362
			Reverse	5′-ACGATTGTGCATCAGCTGA-3′	13,460–13,442
			Probe	5′-FAM-CCGTCTGCG/ZEN/GTATGTGG AAAGGTTATGG-3IABkFQ-3′	13,377–13,404
	China-N	*N*	Forward	5′-GGGGAACTTCTCCTGCTAGAAT-3′	28,881–28,902
			Reverse	5′-CAGACATTTTGCTCTCAAGCTG-3′	28,979–28,958
			Probe	5′-FAM-TTGCTGCTG/ZEN/CTTGACA GATT-3IABkFQ-3′	28,934–28,953
Hong Kong University	HKU-ORF	*ORF1b*	Forward	5′-TGGGGYTTTACRGGTAACCT-3′	18,778–18,797
			Reverse	5′-AACRCGCTTAACAAAGCACTC-3′	18,849–18,872
			Probe	5′-FAM-TAGTTGTGA/ZEN/TGCWA TCATGACTAG-3IABkFQ-3′	18,909–18,889
	HKU-N	*N*	Forward	5′-TAATCAGACAAGGAACTGATTA-3′	29,145–29,166
			Reverse	5′-CGAAGGTGTGACTTCCATG-3′	29,179–29,198
			Probe	5′-FAM-GCAAATTGT/ZEN/GCAATTT GCGG-3IABkFQ-3′	29,254–29,236
US CDC	US-CDC-N1	*N*	Forward	5′-GACCCCAAAATCAGCGAAAT-3′	28,287–28,306
			Reverse	5′-TCTGGTTACTGCCAGTTGAATCTG-3′	28,358–28,335
			Probe	5′-FAM-ACCCCGCAT/ZEN/TACG TTTGGTGGACC-3IABkFQ-3′	28,309–28,332

Coordinates are based on the SARS-CoV-2 Wuhan-Hu-1 genome (*https://www.ncbi.nlm.nih.gov/genbank*; GenBank accession number MN908947.3).
3IABkFQ, 3′ Iowa Black Black Hole Quencher (Integrated DNA Technologies); FAM, 6-carboxyfluorescein; HEX, hexachloro-fluorescein; ZEN, internal ZEN quencher (Integrated DNA Technologies).

Primer and Probe Sets

Eight SARS-CoV-2–specific primer/probe sets developed for real-time RT-PCR COVID-19 diagnostic assays[27] were assessed for use in RT-ddPCR (Table 1). These included the Charité-Berlin *E* gene (E-Sarbeco) set,[28] the Pasteur Institute RdRp IP2 and IP4 sets (IP2 and IP4, respectively),[29] the Chinese Center for Disease Control ORF and *N* gene sets (China-ORF and China-N, respectively),[30] the Hong Kong University ORF and *N* gene sets (HKU-ORF and HKU-N, respectively),[31] and the US-CDC-N1 set.[32] No changes to the sequences or fluorophores were made when transitioning to RT-ddPCR. Fluorescent quenchers originally employed in real-time RT-PCR, however [ie, TAMRA, BlackBerry Quencher (BBQ)] were changed to dark quenchers [ie, IowaBlack Quencher with internal ZEN quencher (3IABkFQ, Integrated DNA Technologies, Coralville, IA)], as recommended for ddPCR (manufacturer's protocol).

SARS-CoV-2 Synthetic RNA Standards

RT-ddPCR assays were evaluated using commercial synthetic SARS-CoV-2 RNA standards comprising six nonoverlapping 5000-base fragments of equal quantities encoding the Wuhan-Hu-1 SARS-CoV-2 genome (Control 2; *https://www.ncbi.nlm.nih.gov/genbank*; GenBank accession number MN908947.3; Twist Biosciences, San Francisco, CA; supplied at approximately 1 million copies/fragment/μL). To avoid degradation, RNA standards were stored at −80°C and thawed only once, immediately before use, to perform the analytical efficiency, precision, analytical sensitivity, and dynamic range analyses described herein. Moreover, to mimic nucleic acid composition of a real biological specimen, all assays employing these standards were supplemented with a consistent, physiologically relevant amount of nucleic acid extracted from pooled remnant SARS-CoV-2–negative nasopharyngeal swabs (Supplemental Figure S1). Briefly, 1-mL aliquots of pooled viral transport medium were extracted on the NucliSens EasyMag (BioMerieux, Marcy-l'Etoile, France), eluted in 60 μL and repooled. The resulting material contained DNA from on average 2200 human cells/μL (as quantified using human RPP30 DNA copy numbers by ddPCR as described in[33]) and 4400 human RNAse P copies/μL extract (as quantified by RT-ddPCR as described in[34]), concentrations that are in line with human DNA and RNA levels recovered on nasopharyngeal swabs.[33,34]

RT-ddPCR for SARS-CoV-2 Quantification

RT-ddPCR reactions were performed by combining relevant SARS-CoV-2 RNA template with target-specific primers and probe (900 nmol/L and 250 nmol/L, respectively; Integrated DNA Technologies, Coralville, IA) (Table 1), One-Step RT-ddPCR Advanced Kit for Probes Supermix, Reverse Transcriptase, and DTT (300 nmol/L) (all from BioRad, Hercules, CA), XhoI restriction enzyme (New England Biolabs, Ipswich, MA), background nucleic acid (for reactions employing synthetic RNA template only, see above), and nuclease free water. Droplets were generated using an Automated Droplet Generator (BioRad) and cycled under primer/probe set–specific conditions (see below) (Figure 1). Analysis was performed on a QX200 Droplet Reader (BioRad) using QuantaSoft software version 1.7.4 (BioRad) where replicate wells were merged prior to analysis.

Thermal Cycling Temperature Optimization

For each primer/probe set, acceptable thermal cycling temperature ranges for reverse transcription and PCR annealing/

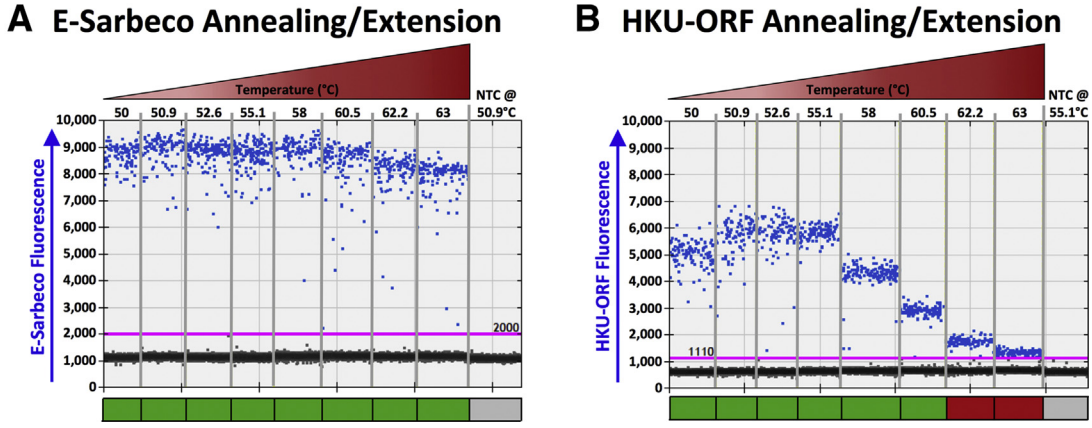

Figure 1 Thermal cycling optimization. **A:** Droplet digital RT-PCR (RT-ddPCR) plots for annealing/extension under a 50°C to 63°C thermal gradient for the E-Sarbeco primer/probe set. A representative RT-ddPCR plot for a no template control (NTC), which only included nontarget DNA/RNA (*Materials and Methods*) at the temperature used in subsequent experiments, is also shown. Positive droplets (**blue**) are above the threshold (**pink line**); negative droplets (**gray**) are below the line. **Colored boxes** below each well indicate whether results met standards for inclusion (**green**) or not (**red**) (*Materials and Methods*). **B:** Same as **A**, but for HKU-ORF primer/probe set.

Table 2 Acceptable Thermal Cycling Temperature Ranges for Primer/Probe Sets Assessed in RT-ddPCR

Acceptable temperature range, °C	E-Sarbeco	IP2	IP4	China-ORF	China-N	HKU-ORF	HKU-N	US-CDC-N1
Reverse transcription	42–49.7	42–51.5	42–50.9	42–51.5	42.7–50.9	42–51.5	42–51.5	42–45.7
Annealing/extension	50–63	50–60.5	50–60.5	50–63	50–60.5	50–60.5	50.9–60.5	50–63

extension were determined by modifying the manufacturer-recommended default conditions, which are 42°C to 50°C for 1 hour (for reverse transcription); 95°C for 10 minutes; 40 cycles of (94°C for 30 seconds followed by 50°C to 63°C for 1 minute); 98°C for 10 minutes, and 4°C infinite hold. To determine acceptable temperature ranges for reverse transcription, a thermal gradient from 42°C to 51.5°C was performed while fixing the annealing/extension step at 52°C. Using the optimized reverse transcription temperature, a thermal gradient from 50°C to 63°C was then performed to identify acceptable annealing/extension temperature ranges. Temperatures that produced insufficient separation of positive from negative droplets or nonspecific amplification were deemed unacceptable, as were those that produced consecutive 95% confidence intervals (CIs) of copy number estimates outside those of the maximal point estimate.

Analytical Efficiency and Precision

The analytical efficiency of each primer/probe set to quantify SARS-CoV-2 RNA by RT-ddPCR was determined using synthetic SARS-CoV-2 RNA standards at 1000 and 100 input copies. A minimum of three (maximum four) technical replicates were performed at each concentration, where results were expressed as the point estimate with 95% total Poisson CI derived from merged replicates. As such, primer/probe sets that yield nonoverlapping 95% total Poisson CIs around the point estimate can be considered significantly different from one another. Analytical efficiency was calculated by dividing the measured SARS-CoV-2 copy number by the expected input copy number and multiplying by 100. Precision was expressed as the coefficient of variation (CV), expressed as a percentage, across technical replicates.

Linear Dynamic Range

The linear dynamic range (LDR) of each primer/probe set of interest was determined across a serial 1:2 dilution series from 114,286 to 1.2 SARS-CoV-2 RNA copies/reaction. This range of concentrations was chosen because it crosses the entire range of recommended input copies for a ddPCR reaction seeking to quantify the target of interest (see the manufacturer's protocol). Reactions were performed in duplicate. The upper limit of quantification and lower limit of quantification (LLOQ) were defined as the upper and lower boundaries of the concentration range over which the relationship between measured and input SARS-CoV-2 RNA copies was linear. The determination was made by iteratively restricting the range of concentrations included in the linear regression of measured versus input SARS-CoV-2 RNA copies to identify the ones which maximized the coefficient of determination (R^2) value and minimized the residuals.

Assay Analytical Sensitivity

Assay analytical sensitivity, defined as the lower limit of detection (LLOD), was determined for primer/probe sets of interest by serially diluting synthetic SARS-CoV-2 RNA standards to between 47.6 and 0.74 SARS-CoV-2 RNA copies/reaction. Between 6 and 18 technical replicates were performed for each dilution, and results were analyzed using probit regression. The LLOD, determined through interpolation of the probit curve, was defined as the concentration of input SARS-CoV-2 RNA in a reaction where the probability of detection was 95%.

SARS-CoV-2 RNA Quantification in Biological Specimens, and Relationship to C_t Value

Optimized RT-ddPCR assays were applied to a convenience sample of 48 consecutive remnant SARS-CoV-2–positive diagnostic nasopharyngeal swab specimens that were originally submitted to the St. Paul's Hospital Virology Laboratory in Vancouver, Canada for diagnostic testing using the Roche cobas SARS-CoV-2 assay. For these samples, total nucleic acids were re-extracted from 250 μL of remnant medium using the BioMerieux NucliSens EasyMag and eluted in 50 μL. Eluates were aliquoted and frozen at −80°C prior to single use. SARS-CoV-2 copy numbers were quantified by RT-ddPCR as described above. As the main goal was to characterize the relationship between C_t values and SARS-CoV-2 RNA levels without confounding by extraction platform, quantity of input material, or SARS-CoV-2 genomic target, these extracts were re-tested using a commercial real-time RT-PCR SARS-CoV-2 diagnostic assay that uses the E-Sarbeco primer/probe set: the LightMix 2019-nCoV real-time RT-PCR assay E-gene target (TIB Molbiol, Berlin, Germany), implemented on LightCycler 480 (Roche Diagnostics, Basel, Switzerland).[35] Finally, to be responsive to a recent recommendation that SARS-CoV-2 viral loads be reported in terms of SARS-CoV-2 RNA copies per human cell equivalents,[9] human cells/microliter of extract were measured by ddPCR as previously described[33] and additionally results reported as SARS-CoV-2 RNA copies/1000 human cells.

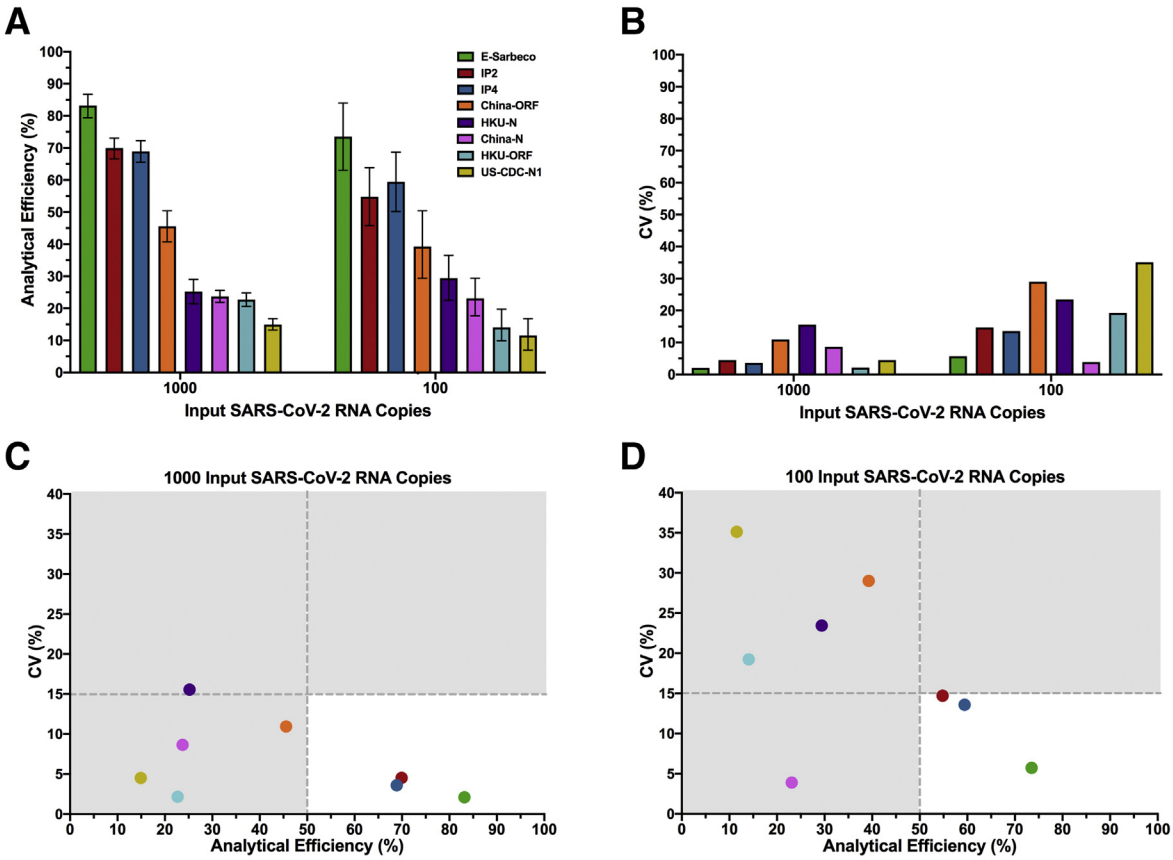

Figure 2 Analytical efficiency and precision of primer/probe sets. **A:** Analytical efficiency of each primer/probe set, calculated as the measured divided by the input SARS-CoV-2 RNA copies multiplied by 100%, is shown for reactions containing 1000 and 100 input copies of synthetic SARS-CoV-2 RNA. Bars represent 95% total Poisson CIs. **B:** Precision of each primer/probe set, defined as the coefficient of variation [expressed as a percentage, coefficient of variation (CV)] of measured copies, is shown for reactions containing 1000 and 100 input copies of synthetic SARS-CoV-2 RNA. **C:** Plotting precision versus analytical efficiency at 1000 input SARS-CoV-2 RNA copies identifies E-Sarbeco, IP2, and IP4 primer/probe sets as having analytical efficiencies >50% and CV (%) <15% (**white background**). All other primer/probe sets had analytical efficiencies <50% and in many cases CV (%) >15% (**gray background**). **D:** Same as **C**, but for 100 input SARS-CoV-2 RNA copies.

Statistical Analysis

SARS-CoV-2 RNA copy numbers were expressed as point estimates with 95% total Poisson CIs derived from merged replicates, calculated using QuantaSoft software version 1.7.4 (Bio-Rad). Assay precision was reported as the CV, expressed as a percentage, across technical replicates. Assay linear dynamic range was determined by identifying the range of concentrations that maximized the coefficient of determination (R^2) and minimized the residuals in the relationship between measured and input SARS-CoV-2 RNA copies. Assay LLOD was determined by probit regression. Correlation between SARS-CoV-2 RNA gene copies measured using different primer/probe sets was determined by Spearman's rho (ρ). Where it was appropriate to measure concordance, Lin's concordance correlation coefficient (ρc) was calculated. The relationship between SARS-CoV-2 viral load as measured by RT-ddPCR and diagnostic test C_t value was evaluated using linear regression. Statistical analyses were performed using GraphPad Prism software version 8 (GraphPad Software, San Diego, CA) or Microsoft Excel software version 14.7.2 (Microsoft, Redmond, WA) with $P < 0.05$ considered statistically significant.

Results

Thermal Cycling Optimization for SARS-CoV-2 Quantification by RT-ddPCR

Eight primer/probe sets originally developed for SARS-CoV-2 diagnostic testing by real-time RT-PCR were evaluated for use in RT-ddPCR (Table 1). Because these primer/probe sets vary in sequence, amplicon length, and SARS-CoV-2 genomic target, the acceptable temperature ranges were first determined for reverse transcription and PCR annealing/extension. Most primer/probe sets were tolerant of a wide temperature range, and background signal was essentially

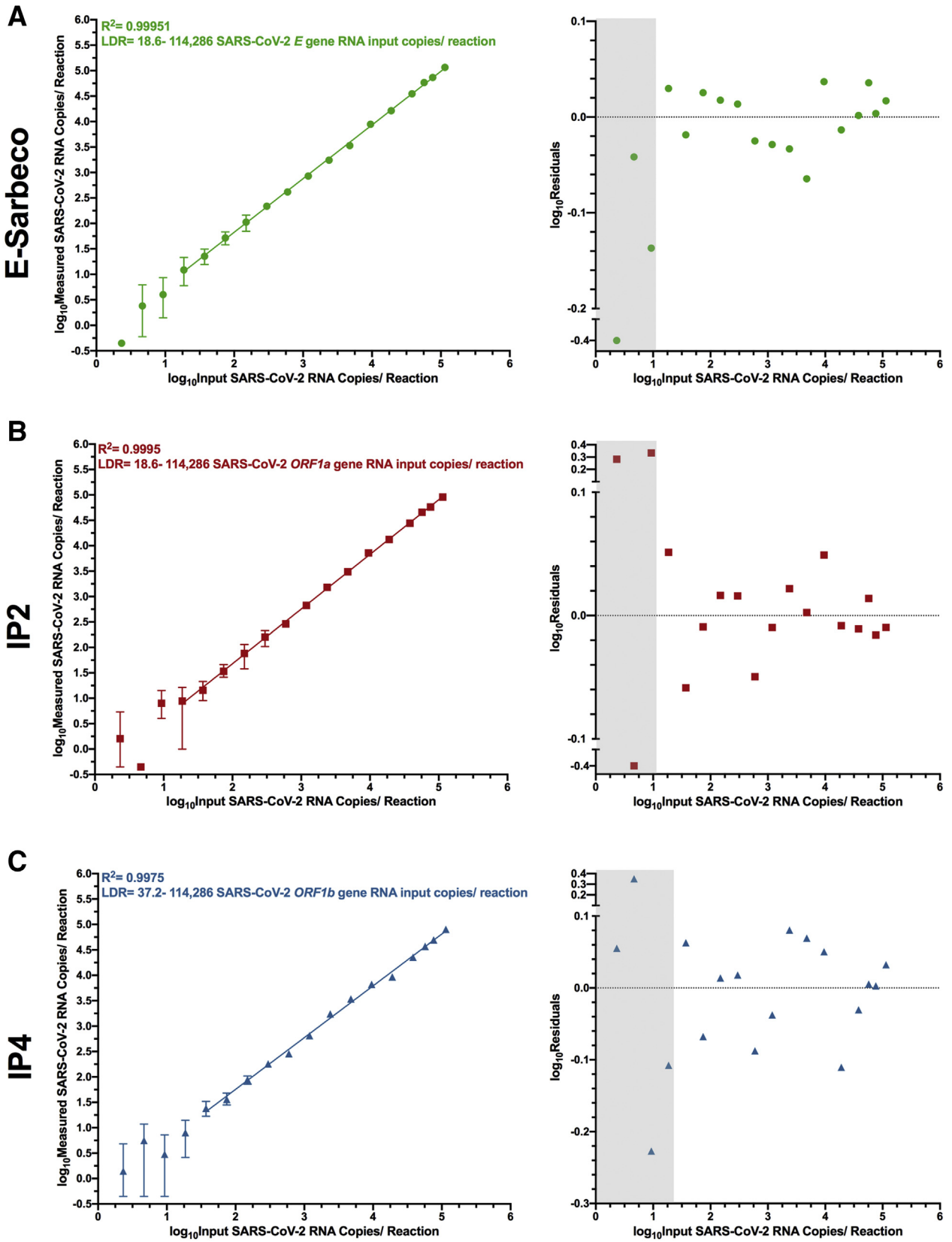
A
E-Sarbeco
R²= 0.99951
LDR= 18.6- 114,286 SARS-CoV-2 E gene RNA input copies/ reaction
log10Measured SARS-CoV-2 RNA Copies/ Reaction
log10Input SARS-CoV-2 RNA Copies/ Reaction
log10Residuals
B
IP2
R²= 0.9995
LDR= 18.6- 114,286 SARS-CoV-2 ORF1a gene RNA input copies/ reaction
log10Measured SARS-CoV-2 RNA Copies/ Reaction
log10Input SARS-CoV-2 RNA Copies/ Reaction
log10Residuals
C
IP4
R²= 0.9975
LDR= 37.2- 114,286 SARS-CoV-2 ORF1b gene RNA input copies/ reaction
log10Measured SARS-CoV-2 RNA Copies/ Reaction
log10Input SARS-CoV-2 RNA Copies/ Reaction
log10Residuals

zero at all temperatures tested (Figure 1). The E-Sarbeco primer/probe set, for example, produced consistent amplitude profiles, copy number estimates, and essentially zero background at annealing/extension temperatures ranging from 50°C to 63°C (Figure 1A) (data not shown). The HKU-ORF primer/probe performed acceptably over a 50°C to 60.5°C annealing/extension range, but positive and negative droplet separation was insufficient at higher temperatures (Figure 1B). Acceptable temperature ranges for each primer/probe set are shown in Table 2. All subsequent experiments were performed at reverse transcription 42.7°C and annealing/extension 50.9°C except those for HKU-ORF and US-CDC-N1, which were performed at reverse transcription 45.7°C and annealing/extension 55.1°C, based on initial, more subjective assessments of RT-ddPCR plot quality.

Analytical Efficiency and Precision of SARS-CoV-2 Quantification by RT-ddPCR

The analytical efficiency of SARS-CoV-2 RNA quantification for each primer/probe set, calculated as the percentage of input viral RNA copies detected by the assay, was next evaluated. Precision, calculated as the dispersion of measured copies around the mean (CV), was also evaluated. Analytical efficiency and precision were evaluated at 1000 and 100 SARS-CoV-2 RNA target input copies. At 1000 input copies, primer/probe set analytical efficiency ranged from 83% (E-Sarbeco) to 15% (US-CDC-N1) (Figure 2A). At 100 copies, the analytical efficiency hierarchy was identical, with values ranging from 74% (E-Sarbeco) to 12% (US-CDC-N1). Of all primer/probe sets evaluated, the E-Sarbeco, IP2, and IP4 sets had the highest analytical efficiencies by a substantial margin. At 1000 and 100 target copies, E-Sarbeco analytical efficiency was 83% (95% total Poisson CI, 79%-87%) and 74% (95% CI, 63%-84%), respectively; IP2 analytical efficiency was 70% (95% CI, 67%-73%) and 55% (95% CI, 46%-64%), respectively; and IP4 analytical efficiency was 69% (95% CI, 66%-72%) and 59% (95% CI, 50%-69%), respectively. By contrast, analytical efficiency of the China-ORF primer/probe set was only 46% and 39% at 1000 and 100 input copies, respectively, and the analytical efficiencies of the remaining sets were <30% regardless of input copy number. Furthermore, while measurement precision generally decreased at the lower template concentration,[36] the E-Sarbeco, IP2, and IP4 primer/probe sets were nevertheless among the most precise, with CVs of <5% at 1000 input copies and <15% at 100 input copies (Figure 2B). Combined analytical efficiency and precision data confirmed E-Sarbeco, IP2, and IP4 as the best-performing primer/probe sets in RT-ddPCR (Figure 2, C and D), so these were moved forward for further characterization.

Reduced Analytical Efficiency When IP2 and IP4 Are Duplexed in RT-ddPCR

Because IP2 and IP4 were originally designed for duplexing in real-time RT-PCR,[29] the authors evaluated them in duplex for RT-ddPCR. Duplexing, however, decreased analytical efficiency, from 70% to 52% (at 1000 input copies) and 55% to 37% (at 100 input copies) for IP2, and from 69% to 49% (at 1000 input copies) and 59% to 38% (at 100 input copies) for IP4 (Supplemental Figure S2A). Duplexing also decreased precision (Supplemental Figure S2B). For IP2, CV increased from 5% to 11% when duplexing at 1000 input copies, and from 15% to 25% when duplexing at 100 input copies. For IP4, CV increased from 4% to 7% (1000 input copies) and from 14% to 21% (100 input copies) with duplexing. Duplexing of these reactions is therefore not recommended in RT-ddPCR, and all IP2 and IP4 assays were performed as single reactions.

LDR and Limits of Quantification of SARS-CoV-2 RNA by RT-ddPCR

Droplet digital PCR can achieve absolute target copy number quantification without a standard curve. To investigate the LDR of quantification of the E-Sarbeco, IP2, and IP4 assays, the authors set up 18 twofold serial dilutions of synthetic SARS-CoV-2 RNA beginning at 114,286 copies/reaction (this copy number is obtained when 120,000 copies are added to a 21-μL reaction, of which 20 μL is used for droplet generation) and ending with 2.32 copies/reaction. This input copy number range crosses nearly the entire manufacturer-recommended template input range for ddPCR reactions seeking to quantify the target of interest, which is 1 to 100,000 copies/reaction (see the manufacturer's protocol).

The LDR of each assay was determined by iteratively restricting the range of concentrations included in the linear regression of measured versus input SARS-CoV-2 RNA copies to identify the range that maximized the R^2 value and minimized the residuals. For E-Sarbeco, the regression spanning 18.6 to 114,286 input SARS-CoV-2 RNA copies

Figure 3 Linear dynamic range (LDR) of E-Sarbeco, IP2, and IP4 droplet digital RT-PCR (RT-ddPCR) assays. **A: Left:** $\log_{10}$ measured SARS-CoV-2 RNA copies over serial dilutions of synthetic SARS-CoV-2 RNA standards ranging from 114,286 to 2.32 copies/reaction (shown as $\log_{10}$ values), using the E-Sarbeco primer/probe set. Error bars indicate 95% total Poisson CIs for two merged replicates, where in some cases error bars are too small to visualize. The regression line joins all data points included in the LDR, where the lower boundary of the LDR represents the lower limit of quantification of the assay. Data points that yielded undetectable measurements are set arbitrarily to $-0.35\log_{10}$ measured copies/reaction for visualization. **Right:** $\log_{10}$ residuals, calculated as $\log_{10}$ measured SARS-CoV-2 RNA copies/reaction minus $\log_{10}$ calculated SARS-CoV-2 RNA copies/reaction from the LDR regression. **Gray shading** indicates data points outside the LDR. Residuals for data points that yielded undetectable measurements are arbitrarily set to −0.4 for visualization. **B:** Same as **A**, but for the IP2 primer/probe set. **C:** Same as **A**, but for the IP4 primer/probe set.

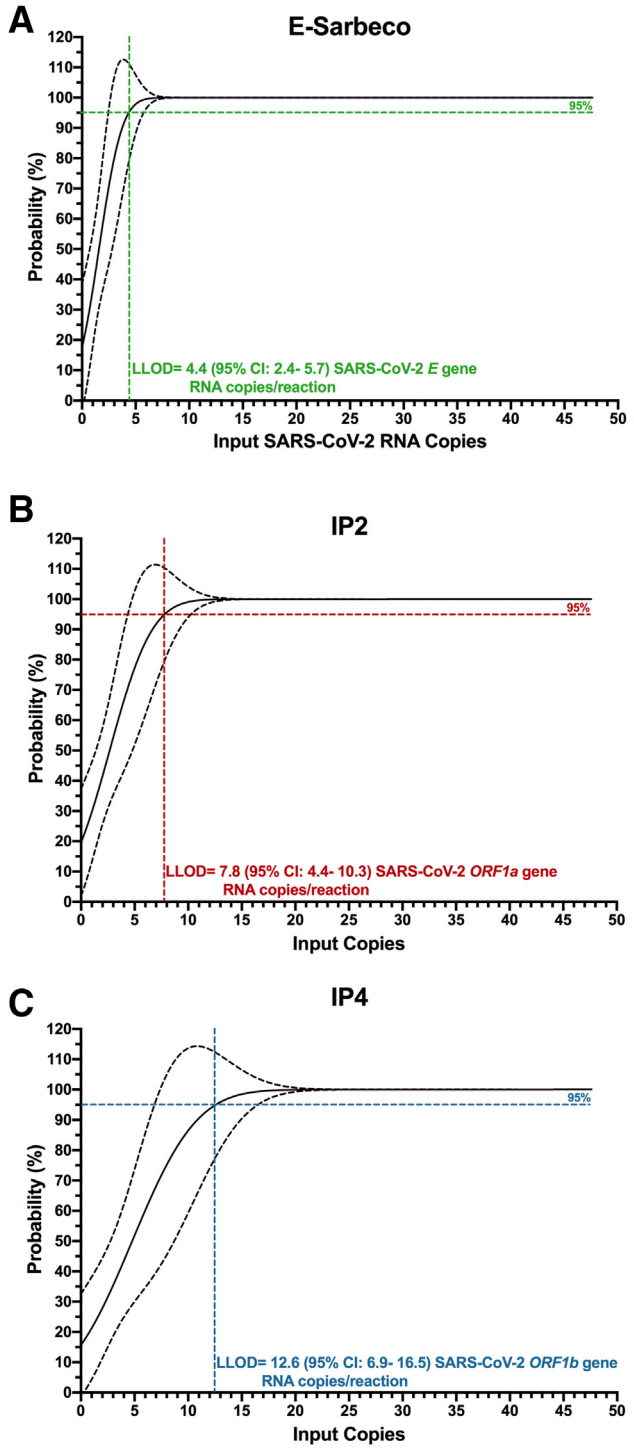

Figure 4 Lower limit of detection (LLOD) of the E-Sarbeco, IP2, and IP4 droplet digital RT-PCR (RT-ddPCR) assays. **A:** The probability of detecting SARS-CoV-2 RNA (%) in 1:2 in serial dilutions of synthetic SARS-CoV-2 RNA from 47.6 to 0.74 input copies/reaction using the E-Sarbeco primer/probe set is analyzed using probit regression (**solid black line**; **dashed line** denotes the 95% CI). The LLOD, defined as the concentration of SARS-CoV-2 RNA in a reaction where the probability of detection in the assay was 95%, was interpolated from the probit curve and is shown as a **colored dashed line**. **B:** Same as **A**, but for the IP2 primer/probe set. **C:** Same as **A**, but for the IP4 primer/probe set.

per reaction, an approximately 6100-fold concentration range, yielded an R^2 value of 0.9995 (Figure 3A). Restricting the linear regression to this range also minimized the residuals of all included data points to $\pm 0.065 \log_{10}$ copies/reaction (Figure 3A). The IP2 assay, although less efficient than E-Sarbeco, had the same estimated LDR of 18.6 to 114,286 input copies/reaction (Figure 3B). This produced an R^2 value of 0.9995 and residuals within $\pm 0.065 \log_{10}$ copies/reaction across the LDR (Figure 3B). The LDR of IP4 was estimated as 37.2 to 114,286 input copies/reaction, an approximately 3000-fold range, which yielded an $R^2 = 0.9975$ and produced residuals within $\pm 0.11 \log_{10}$ copies/reaction across this range (Figure 3C). For all three assays, 114,286 input copies/reaction should be considered a conservative estimate of the upper limit of quantification, because saturation of the RT-ddPCR reaction or loss of linearity was still not achieved at this concentration.

LLOD of SARS-CoV-2 RNA by RT-ddPCR

The authors next determined the LLOD of the E-Sarbeco, IP2, and IP4 RT-ddPCR assays (Figure 4). Probit regression analysis applied to serial dilutions of synthetic SARS-CoV-2 RNA standards revealed the E-Sarbeco RT-ddPCR assay to be the most analytically sensitive of the three, which is consistent with it also having the highest analytical efficiency. Specifically, the estimated LLOD of the E-Sarbeco assay was 4.4 (95% CI, 2.4-5.7) SARS-CoV-2 RNA copies/reaction (Figure 4A). The estimated LLOD of the IP2 assay was 7.8 (95% CI, 4.4-10.3) SARS-CoV-2 RNA copies/reaction (Figure 4B), whereas that of IP4 was 12.6 (95% CI, 6.9-16.5) SARS-CoV-2 RNA copies per reaction (Figure 4C).

SARS-CoV-2 Viral Loads in Biological Samples

SARS-CoV-2 viral loads were measured in 48 confirmed SARS-CoV-2–positive samples using the E-Sarbeco, IP2, and IP4 primer/probe sets (note that samples with original diagnostic test C_t values <19 required RNA extracts to be diluted up to 1:200 prior to quantification to ensure that input copies measurements fell within each assay's LDR). The results revealed that SARS-CoV-2 RNA in these biological samples varied over a 6.2 $\log_{10}$ range (Figure 5A). Average copy numbers measured using the E-Sarbeco assay (which targets the *E* gene) were higher than those using the IP2 and IP4 assays (which target *ORF1a* and *ORF1b*, respectively) (Figure 5A). This is consistent with assay analytical efficiency (Figure 2) and *in vivo* coronavirus RNA expression patterns, where transcripts covering the 3′ end of the genome are more abundant than those covering the 5′ end.[37–40] Specifically, the median *E* gene copy number was 5.1 [interquartile range (IQR), 3.9 to 5.7] $\log_{10}$ copies/μL extract compared with a median of 4.9 (IQR, 3.9

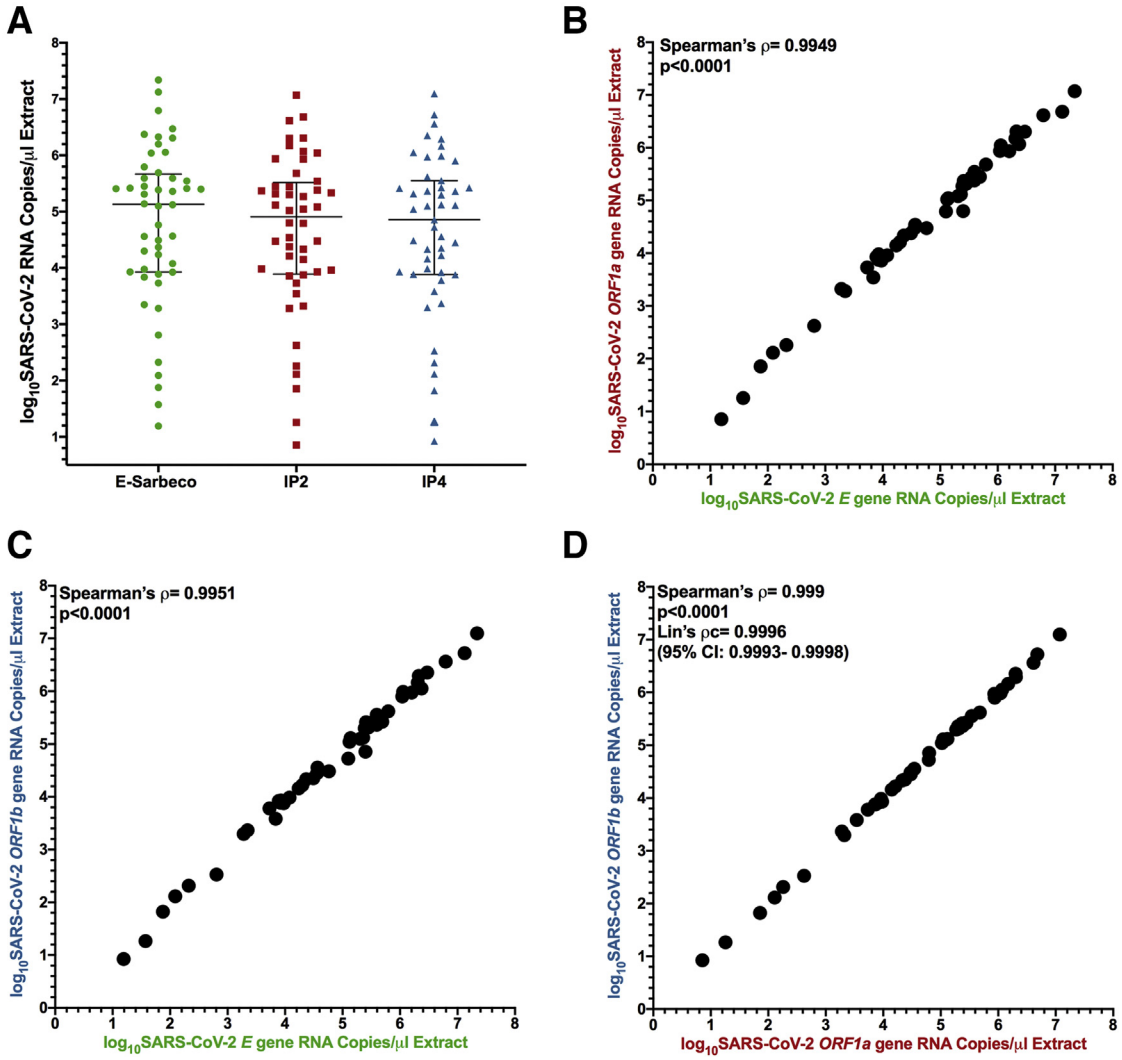

Figure 5 Log_{10}SARS-CoV-2 RNA loads in diagnostic specimens. **A:** SARS-CoV-2 *E* (**green circles**), *ORF1a* (**red squares**), and *ORF1b* (**blue triangles**) gene copy numbers, expressed as RNA copies/microliter of nucleic acid extract. Line and bars indicate median and interquartile range, respectively. **B:** Spearman's correlation (ρ) between log_{10} SARS-CoV-2 *E* and *ORF1a* gene RNA copies/microliter extract. **C:** Spearman's correlation (ρ) between log_{10} SARS-CoV-2 *E* and *ORF1b* gene RNA copies/microliter extract. **D:** Spearman's correlation (ρ) and Lin's concordance correlation (ρc) between log_{10} SARS-CoV-2 *ORF1a* and *ORF1b* gene RNA copies/microliter extract.

to 5.5) log_{10} copies/μL extract for the IP2 target, and a median of 4.9 (IQR, 3.9 to 5.6) log_{10} copies/μL extract for the IP4 target. SARS-CoV-2 *E* gene, IP2, and IP4 copy numbers in biological samples correlated strongly with one another (Spearman's $\rho > 0.99$; $P < 0.0001$ for all pairwise analyses) (Figure 5, B–D). Consistent with comparable *ORF1a* and *ORF1b* RNA transcript levels *in vivo*,[37,38,40] IP2 and IP4 copy numbers were also highly concordant [Lin's concordance correlation coefficient, $\rho c = 0.9996$ (95% CI, 0.9993-0.9998)] (Figure 5D). Based on a recent recommendation,[9] the authors also report their results in terms of SARS-CoV-2 RNA copies per human cell equivalents: results for E-Sarbeco spanned a sevenfold range from 1.05 to 7.3 log_{10} SARS-CoV-2 RNA copies/1000 human cells, with IP2 and IP4 log_{10} copy numbers lower, as expected (Supplemental Figure S3A). The Spearman's correlation between absolute and human cell–normalized viral loads was strong ($P < 0.0001$) (Supplemental Figure S3B), which is consistent with the assumption that the amount of biological material collected by nasopharyngeal swabs is relatively consistent.

Inferring SARS-CoV-2 Viral Loads from Diagnostic C_t Values

Finally, the relationship between C_t values produced by a commercial COVID-19 diagnostic platform and SARS-CoV-2 RNA copy numbers was characterized. The authors selected the LightMix 2019-nCoV real-time RT-PCR assay, E-gene target (TIB Molbiol), implemented on a LightCycler 480 (Roche Diagnostics) because commercial diagnostic reagents comprising the E-Sarbeco primer/probe

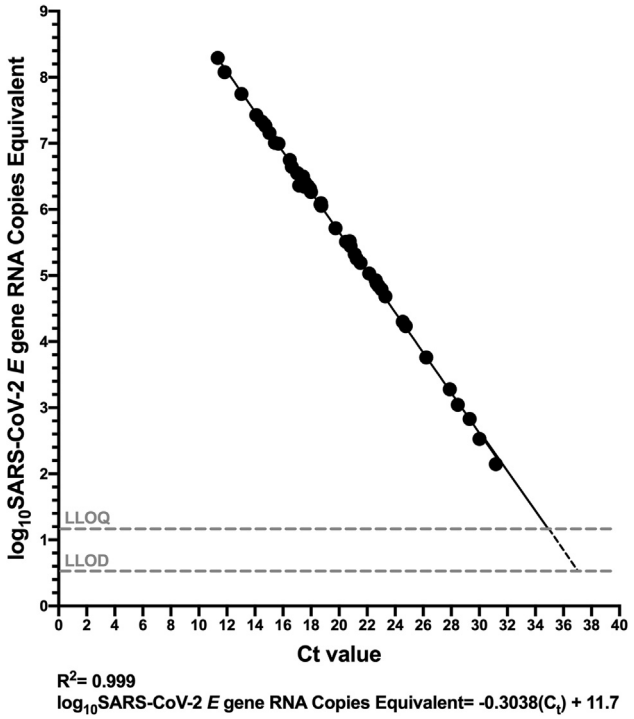

Figure 6 Relationship between SARS-CoV-2 RNA copies equivalent and diagnostic test cycle threshold (C_t) value. C_t value, determined using the LightMix 2019-nCoV real-time RT-PCR assay (*E* gene target) is plotted against $\log_{10}$ SARS-CoV-2 *E* gene RNA copies equivalent, which represents the number of SARS-CoV-2 RNA copies measured by droplet digital RT-PCR (RT-ddPCR) in 9 μL of extract (the template volume in the LightMix assay). The linear regression (**solid black line**) transitions to a **dashed line** below the LLOQ.

set exist for this platform[28] and because it takes purified nucleic acids as input, thereby allowing direct comparison of results from the same starting material (real-time RT-PCR platforms that take biological material as input are suboptimal for such a comparison because the onboard extraction introduces an additional variable). Because the C_t values reported for the LightMix assay are based on a 9-μL extract input volume in the authors' laboratory,[35] their primary analysis reported RT-ddPCR results in terms of SARS-CoV-2 copies equivalent (ie, SARS-CoV-2 copies in 9 μL of extract), to allow direct conversion of C_t values to absolute viral copy numbers.

Sample C_t values ranged from 11.34 to 31.18 [median 18.69 (IQR, 16.73 to 22.69)] using the LightMix assay. The relationship between C_t value and SARS-CoV-2 RNA copy numbers was log-linear, with an $R^2 = 0.9990$ (Figure 6). Despite this strong relationship, inspection of the residuals nevertheless suggested modest departures from log-linearity at the extremes of the linear range (Supplemental Figure S4). The relationship between C_t value and absolute SARS-CoV-2 *E* gene copies can thus be given by $\log_{10}$ SARS-CoV-2 *E* gene copies equivalent $= -0.3038\ C_t + 11.7$ (Figure 6). That is, a C_t value of 20 corresponds to 453,942 (ie, 5.66 $\log_{10}$) SARS-CoV-2 RNA copies, whereas a C_t value of 30 corresponds to 416 (ie, 2.62 $\log_{10}$) viral copies. This equation also predicts that the C_t values corresponding to the LLOQ and LLOD of the E-Sarbeco RT-ddPCR assays are 34.8 and 36.84, respectively. When measured SARS-CoV-2 RNA copy numbers are expressed as human cell–normalized viral loads, the relationship with the C_t value is given by $\log_{10}$ SARS-CoV-2 *E* gene copies/1000 human cells $= -0.3041\ C_t + 10.8$ (Supplemental Figure S5). An extract that yielded a C_t value of 20, therefore, is estimated to have contained 48,978 (ie, 4.69 $\log_{10}$) SARS-CoV-2 RNA copies/1000 human cells, whereas one with a C_t value of 30 is estimated to have contained 45 (ie, 1.66 $\log_{10}$) copies/1000 human cells.

Discussion

Although real-time and droplet digital RT-PCR both employ target-specific primers coupled with fluorescence-based amplicon detection, there are key differences in reaction chemistry (eg, RT-ddPCR reagents must be compatible with water-in-oil droplet partitioning) and probe chemistry (eg, whereas real-time RT-PCR uses fluorescent quenchers, ddPCR typically uses dark quenchers). As a result, assays developed for one platform may not always translate seamlessly to the other. For example, ddPCR probes should ideally not have a guanine at their 5′ end because this quenches the fluorescence signal even following hydrolysis (see the manufacturer's protocol), but the HKU-N probe has a G at its 5′ end (Table 1).

It is perhaps therefore not surprising that the overall performance of the eight primer/probe sets in RT-ddPCR did not exactly mirror that in real-time RT-PCR.[41,42] Nevertheless, E-Sarbeco, IP2, and IP4, which represented the most efficient and precise primer/probe sets for SARS-CoV-2 RNA quantification by RT-ddPCR, are also among the most efficient in real-time RT-PCR.[41,42] The authors' results also confirm previous reports of the E-Sarbeco primer/probe set performing well in RT-ddPCR.[11,23] Other primer/probe sets, however, notably US CDC-N1, HKU-ORF, and China-ORF, did not perform as well in the authors' RT-ddPCR assay compared with a previous report.[11] One key difference is that, whereas the authors used sequence-specific reverse transcription (with the reverse primer) in a one-step RT-ddPCR reaction, the previous study featured an independent reverse transcription reaction primed with random hexamers and oligo dT—which can yield higher efficiency than sequence-specific priming[36,43–45]—to generate cDNA for input into a ddPCR reaction. This is the first study to evaluate IP2 or IP4 primer/probe sets in RT-ddPCR.

The analytical sensitivities of the RT-ddPCR assays reported here are nevertheless comparable to existing estimates. The limit of detection of the BioRad SARS-CoV-2

ddPCR Kit, for example, is estimated at 150 copies/mL (manufacturer's protocol), which is comparable to the authors' E-Sarbeco RT-ddPCR assay (estimated at 75.8 copies/mL assuming 100% extraction efficiency). Similarly, the LLODs of the TargetingOne (Beijing, China) COVID-19 digital PCR detection kit[24] and a multiplex assay that included the E-Sarbeco primer/probe set[23] were reported at 10 copies/test and 5 copies/reaction, respectively, both comparable to the LLOD determined here. Although a number of studies have reported that RT-ddPCR can detect SARS-CoV-2 RNA in low viral load clinical samples with higher sensitivity than real-time RT-PCR,[12,21,22,24–26] the current study was not designed to evaluate this. The estimated LLOD of 4.4 copies/reaction by RT-ddPCR using the E-Sarbeco primer/probe set (Figure 4) is in fact comparable to the LLOD reported by the manufacturers for many real-time RT-PCR–based COVID-19 diagnostic assays,[46] though it is important to note that these lower limits are theoretical. In practice, various factors impact assay efficiency, most notably the presence of PCR inhibitors in biological samples that are not removed by the extraction process,[47] as well as the efficiency of the extraction process itself. In theory, the sample partitioning and end-point measurement used in ddPCR should make this technology more robust to small quantities of inhibitors than real-time PCR technologies that rely on initial detection of fluorescent signal above background ([48–51] and the manufacturer's protocol), though all platforms will be affected by nucleic acid extraction efficiency.

The ability to quantify SARS-CoV-2 viral loads in biological samples can advance our understanding of COVID-19 biology, and RT-ddPCR offers an attractive platform.[7,8] The observation that, in a small convenience sample, both absolute and human cell–normalized[9] SARS-CoV-2 loads spanned more than a 6 $\log_{10}$ range confirms an enormous viral load range *in vivo*[52] and suggests that some of the high viral load samples measured here were from individuals with early and progressive infection[24,53–55] or who were experiencing severe disease,[7,8] though clinical information was unknown. The ability to quantify SARS-CoV-2 viral loads in biological samples—particularly when these are normalized to the amount of human biological material collected (as nasopharyngeal swabs, eg, are stored in variable amounts of viral transport medium, making it difficult to standardize viral copy numbers volumetrically across studies, laboratories, and over time)—opens numerous opportunities to advance our understanding of SARS-CoV-2 biology. Accurate viral load measurements for example can enhance our understanding of the impact of emerging SARS-CoV-2 sequence variants on transmissibility and virulence, and provide a powerful tool to evaluate the ability of novel therapeutic candidates to suppress viral replication, and by extension transmission. Furthermore, the authors' equation relating C_t values derived from a commercial diagnostic assay and SARS-CoV-2 RNA copy number means that existing diagnostic test results can be converted to viral loads without re-testing samples. Although calibration of viral load measurements against all real-time RT-PCR platforms is beyond the authors' scope, this is achievable and in some cases data may already be available.[24]

Some limitations merit mention. Only eight commonly used SARS-CoV-2–specific primer/probe sets were tested, and others may exist that adapt well to RT-ddPCR. The authors' assay performance estimates should be considered approximate, because the manufacturer-reported concentration of the synthetic SARS-CoV-2 RNA standards used in this study may vary by up to 20% error (Twist Bioscience, personal communication). Moreover, the authors solely evaluated a one-step RT-ddPCR protocol, and therefore assay performance estimates will likely differ from protocols that feature independent cDNA generation followed by ddPCR. The upper boundary of the linear dynamic range of the E-Sarbeco, IP2, and IP4 RT-ddPCR assays could not be precisely defined because linearity was maintained at the maximum input of 114,286 target copies/reaction, which already exceeds the manufacturer's estimated upper range of quantification in a ddPCR reaction (manufacturer protocol). Our convenience panel of 48 SARS-CoV-2–positive diagnostic specimens also likely did not capture the full range of biological variation in viral loads, though data from larger cohorts[52] suggests that it was reasonably comprehensive. The authors also acknowledge that there is measurement uncertainty with real-time RT-PCR C_t values that may subtly affect the linear relationship between C_t value and RT-ddPCR–derived SARS-CoV-2 viral load described here. Importantly, however, measuring quantitative viral loads enables an objective evaluation of the RT-PCR C_t value cutoffs used to distinguish positive, indeterminate, and negative results—thresholds that can vary across assays and laboratories. Finally, the authors' estimates of assay performance may not completely reflect those of the entire diagnostic process, because the nucleic acid extraction step introduces additional inefficiencies.

In conclusion, primer/probe sets used in real-time RT-PCR–based COVID-19 diagnostic tests can be migrated to RT-ddPCR to achieve SARS-CoV-2 RNA quantification with varying analytical efficiency, precision, and sensitivity. Of the primer/probe sets tested, the E-Sarbeco, IP2, and IP4 sets performed best, where LLOQ and LLOD estimates for the E-Sarbeco assay (18.6 and 4.4 copies/reaction, respectively) indicated that RT-ddPCR and real-time RT-PCR have comparable sensitivity. Mathematical inference of SARS-CoV-2 copy numbers from COVID-19 diagnostic test C_t values, made possible via the type of calibration performed in the present study, will allow the wealth of existing diagnostic test data to be harnessed to answer foundational questions in SARS-CoV-2 biology.

Supplemental Data

Supplemental material for this article can be found at *http://doi.org/10.1016/j.jmoldx.2021.04.014*.

References

1. Mellors JW, Rinaldo CR Jr, Gupta P, White RM, Todd JA, Kingsley LA: Prognosis in HIV-1 infection predicted by the quantity of virus in plasma. Science 1996, 272:1167−1170
2. Mellors JW: Viral-load tests provide valuable answers. Sci Am 1998, 279:90−93
3. Riddler SA, Mellors JW: HIV-1 viral dynamics and viral load measurement: implications for therapy. AIDS Clin Rev 1997:47−65
4. Mellors JW, Muñoz A, Giorgi JV, Margolick JB, Tassoni CJ, Gupta P, Kingsley LA, Todd JA, Saah AJ, Detels R, Phair JP, Rinaldo CR Jr: Plasma viral load and CD4+ lymphocytes as prognostic markers of HIV-1 infection. Ann Intern Med 1997, 126: 946−954
5. Durante-Mangoni E, Zampino R, Portella G, Adinolfi LE, Utili R, Ruggiero G: Correlates and prognostic value of the first-phase hepatitis C virus RNA kinetics during treatment. Clin Infect Dis 2009, 49:498−506
6. Chen G, Lin W, Shen F, Iloeje UH, London WT, Evans AA: Past HBV viral load as predictor of mortality and morbidity from HCC and chronic liver disease in a prospective study. Am J Gastroenterol 2006, 101:1797−1803
7. Veyer D, Kernéis S, Poulet G, Wack M, Robillard N, Taly V, L'Honneur AS, Rozenberg F, Laurent-Puig P, Bélec L, Hadjadj J, Terrier B, Péré H: Highly sensitive quantification of plasma SARS-CoV-2 RNA sheds light on its potential clinical value. Clin Infect Dis 2020:ciaa1196
8. Bermejo-Martin JF, González-Rivera M, Almansa R, Micheloud D, Tedim AP, Domínguez-Gil M, et al: Viral RNA load in plasma is associated with critical illness and a dysregulated host response in COVID-19. medRxiv 2020. doi:10.1101/2020.08.25.20154252
9. Han MS, Byun JH, Cho Y, Rim JH: RT-PCR for SARS-CoV-2: quantitative versus qualitative. Lancet Infect Dis 2021, 21:165
10. Lescure FX, Bouadma L, Nguyen D, Parisey M, Wicky PH, Behillil S, Gaymard A, Bouscambert-Duchamp M, Donati F, Le Hingrat Q, Enouf V, Houhou-Fidouh N, Valette M, Mailles A, Lucet JC, Mentre F, Duval X, Descamps D, Malvy D, Timsit JF, Lina B, van-der-Werf S, Yazdanpanah Y: Clinical and virological data of the first cases of COVID-19 in Europe: a case series. Lancet Infect Dis 2020, 20:697−706
11. Liu X, Feng J, Zhang Q, Guo D, Zhang L, Suo T, Hu W, Guo M, Wang X, Huang Z, Xiong Y, Chen G, Chen Y, Lan K: Analytical comparisons of SARS-COV-2 detection by qRT-PCR and ddPCR with multiple primer/probe sets. Emerg Microbes Infect 2020, 9:1175−1179
12. Suo T, Liu X, Feng J, Guo M, Hu W, Guo D, Ullah H, Yang Y, Zhang Q, Wang X, Sajid M, Huang Z, Deng L, Chen T, Liu F, Xu K, Liu Y, Zhang Q, Liu Y, Xiong Y, Chen G, Lan K, Chen Y: ddPCR: a more accurate tool for SARS-CoV-2 detection in low viral load specimens. Emerg Microbes Infect 2020, 9:1259−1268
13. Salemi R, Falzone L, Madonna G, Polesel J, Cinà D, Mallardo D, Ascierto PA, Libra M, Candido S: MMP-9 as a candidate marker of response to BRAF inhibitors in melanoma patients with BRAF(V600E) mutation detected in circulating-free DNA. Front Pharmacol 2018, 9:856
14. Findlay SD, Vincent KM, Berman JR, Postovit LM: A digital PCR-based method for efficient and highly specific screening of genome edited cells. PLoS One 2016, 11:e0153901
15. Lillsunde Larsson G, Helenius G: Digital droplet PCR (ddPCR) for the detection and quantification of HPV 16, 18, 33 and 45 - a short report. Cell Oncol (Dordr) 2017, 40:521−527
16. Stevenson A, Wakeham K, Pan J, Kavanagh K, Millan D, Bell S, McLellan D, Graham SV, Cuschieri K: Droplet digital PCR quantification suggests that higher viral load correlates with improved survival in HPV-positive oropharyngeal tumours. J Clin Virol 2020, 129:104505
17. Cao WW, He DS, Chen ZJ, Zuo YZ, Chen X, Chang YL, Zhang ZG, Ye L, Shi L: Development of a droplet digital PCR for detection and quantification of porcine epidemic diarrhea virus. J Vet Diagn Invest 2020, 32:572−576
18. Persson S, Eriksson R, Lowther J, Ellström P, Simonsson M: Comparison between RT droplet digital PCR and RT real-time PCR for quantification of noroviruses in oysters. Int J Food Microbiol 2018, 284:73−83
19. Pinheiro-de-Oliveira TF, Fonseca AA Jr, Camargos MF, Laguardia-Nascimento M, de Oliveira AM, Cottorello ACP, Goes-Neto A, Barbosa-Stancioli EF: Development of a droplet digital RT-PCR for the quantification of foot-and-mouth virus RNA. J Virol Methods 2018, 259:129−134
20. Bruner KM, Wang Z, Simonetti FR, Bender AM, Kwon KJ, Sengupta S, Fray EJ, Beg SA, Antar AAR, Jenike KM, Bertagnolli LN, Capoferri AA, Kufera JT, Timmons A, Nobles C, Gregg J, Wada N, Ho YC, Zhang H, Margolick JB, Blankson JN, Deeks SG, Bushman FD, Siliciano JD, Laird GM, Siliciano RF: A quantitative approach for measuring the reservoir of latent HIV-1 proviruses. Nature 2019, 566:120−125
21. Dong L, Zhou J, Niu C, Wang Q, Pan Y, Sheng S, Wang X, Zhang Y, Yang J, Liu M, Zhao Y, Zhang X, Zhu T, Peng T, Xie J, Gao Y, Wang D, Dai X, Fang X: Highly accurate and sensitive diagnostic detection of SARS-CoV-2 by digital PCR. Talanta 2021, 224:121726
22. Falzone L, Musso N, Gattuso G, Bongiorno D, Palermo CI, Scalia G, Libra M, Stefani S: Sensitivity assessment of droplet digital PCR for SARS-CoV-2 detection. Int J Mol Med 2020, 46:957−964
23. de Kock R, Baselmans M, Scharnhorst V, Deiman B: Sensitive detection and quantification of SARS-CoV-2 by multiplex droplet digital RT-PCR. Eur J Clin Microbiol Infect Dis 2021, 40:807−813
24. Yu F, Yan L, Wang N, Yang S, Wang L, Tang Y, Gao G, Wang S, Ma C, Xie R, Wang F, Tan C, Zhu L, Guo Y, Zhang F: Quantitative detection and viral load analysis of SARS-CoV-2 in infected patients. Clin Infect Dis 2020, 71:793−798
25. Alteri C, Cento V, Antonello M, Colagrossi L, Merli M, Ughi N, Renica S, Matarazzo E, Di Ruscio F, Tartaglione L, Colombo J, Grimaldi C, Carta S, Nava A, Costabile V, Baiguera C, Campisi D, Fanti D, Vismara C, Fumagalli R, Scaglione F, Epis OM, Puoti M, Perno CF: Detection and quantification of SARS-CoV-2 by droplet digital PCR in real-time PCR negative nasopharyngeal swabs from suspected COVID-19 patients. PLoS One 2020, 15:e0236311
26. Dang Y, Liu N, Tan C, Feng Y, Yuan X, Fan D, Peng Y, Jin R, Guo Y, Lou J: Comparison of qualitative and quantitative analyses of COVID-19 clinical samples. Clin Chim Acta 2020, 510:613−616
27. World-Health-Organization: Summary of Available SARS-CoV-2 RT-PCR Protocols. Geneva, Switzerland: World Health Organiation, 2020
28. Corman VM, Landt O, Kaiser M, Molenkamp R, Meijer A, Chu DK, Bleicker T, Brünink S, Schneider J, Schmidt ML, Mulders DG, Haagmans BL, van der Veer B, van den Brink S, Wijsman L, Goderski G, Romette JL, Ellis J, Zambon M, Peiris M, Goossens H, Reusken C, Koopmans MP, Drosten C: Detection of 2019 novel coronavirus (2019-nCoV) by real-time RT-PCR. Euro Surveill 2020, 25:2000045
29. Institut-Pasteur-Paris: Protocol: Real-Time RT-PCR Assays for the Detection of SARS-CoV-2; 2020
30. Chinese-National-Institute-for-Viral-Disease-Control-and-Prevention: Specific Primers and Probes for Detection of 2019 Novel Coronavirus; 2020
31. School-of-Public-Health-LKS-Faculty-of-Medicine-University-of-Hong-Kong: Detection of 2019 Novel Coronavirus (2019-nCoV) in Suspected Human Cases by RT-PCR; 2020

32. Centers-for-Disease-Control-and-Prevention: CDC 2019-Novel Coronavirus (2019-nCoV) Real-Time RT-PCR Diagnostic Panel; 2020
33. Kinloch NN, Ritchie G, Brumme CJ, Dong W, Dong W, Lawson T, Jones RB, Montaner JSG, Leung V, Romney MG, Stefanovic A, Matic N, Lowe CF, Brumme ZL: Suboptimal biological sampling as a probable cause of false-negative COVID-19 diagnostic test results. J Infect Dis 2020, 222:899–902
34. Kinloch NN, Shahid A, Ritchie G, Dong W, Lawson T, Montaner JSG, Romney MG, Stefanovic A, Matic N, Brumme CJ, Lowe CF, Brumme ZL, Leung V: Evaluation of nasopharyngeal swab collection techniques for nucleic acid recovery and participant experience: recommendations for COVID-19 diagnostics. Open Forum Infect Dis 2020, 7:ofaa488
35. Matic N, Stefanovic A, Leung V, Lawson T, Ritchie G, Li L, Champagne S, Romney MG, Lowe CF: Practical challenges to the clinical implementation of saliva for SARS-CoV-2 detection. Eur J Clin Microbiol Infect Dis 2021, 40:447–450
36. Schwaber J, Andersen S, Nielsen L: Shedding light: the importance of reverse transcription efficiency standards in data interpretation. Biomol Detect Quantif 2019, 17:100077
37. Kim D, Lee JY, Yang JS, Kim JW, Kim VN, Chang H: The architecture of SARS-CoV-2 transcriptome. Cell 2020, 181:914–921.e910
38. Irigoyen N, Firth AE, Jones JD, Chung BY, Siddell SG, Brierley I: High-resolution analysis of coronavirus gene expression by RNA sequencing and ribosome profiling. PLoS Pathog 2016, 12:e1005473
39. Dimmock NJ, Easton AJ, Leppard KN: Introduction to Modern Virology. 6 ed. Malden, MA: Blackwell Publishing, 2007
40. Davidson AD, Williamson MK, Lewis S, Shoemark D, Carroll MW, Heesom KJ, Zambon M, Ellis J, Lewis PA, Hiscox JA, Matthews DA: Characterisation of the transcriptome and proteome of SARS-CoV-2 reveals a cell passage induced in-frame deletion of the furin-like cleavage site from the spike glycoprotein. Genome Med 2020, 12:68
41. Vogels CBF, Brito AF, Wyllie AL, Fauver JR, Ott IM, Kalinich CC, et al: Analytical sensitivity and efficiency comparisons of SARS-CoV-2 RT-qPCR primer-probe sets. Nat Microbiol 2020, 5: 1299–1305
42. Etievant S, Bal A, Escuret V, Brengel-Pesce K, Bouscambert M, Cheynet V, Generenaz L, Oriol G, Destras G, Billaud G, Josset L, Frobert E, Morfin F, Gaymard A: Performance assessment of SARS-CoV-2 PCR assays developed by WHO referral laboratories. J Clin Med 2020, 9:1871
43. Bustin SA, Benes V, Nolan T, Pfaffl MW: Quantitative real-time RT-PCR–a perspective. J Mol Endocrinol 2005, 34:597–601
44. Sanders R, Mason DJ, Foy CA, Huggett JF: Evaluation of digital PCR for absolute RNA quantification. PLoS One 2013, 8:e75296
45. Levesque-Sergerie JP, Duquette M, Thibault C, Delbecchi L, Bissonnette N: Detection limits of several commercial reverse transcriptase enzymes: impact on the low- and high-abundance transcript levels assessed by quantitative RT-PCR. BMC Mol Biol 2007, 8:93
46. Lai CC, Wang CY, Ko WC, Hsueh PR: In vitro diagnostics of coronavirus disease 2019: technologies and application. J Microbiol Immunol Infect 2021, 54:164–174
47. Carvalhais V, Delgado-Rastrollo M, Melo LD, Cerca N: Controlled RNA contamination and degradation and its impact on qPCR gene expression in S. epidermidis biofilms. J Microbiol Methods 2013, 95: 195–200
48. Rački N, Dreo T, Gutierrez-Aguirre I, Blejec A, Ravnikar M: Reverse transcriptase droplet digital PCR shows high resilience to PCR inhibitors from plant, soil and water samples. Plant Methods 2014, 10:42
49. Devonshire AS, Sanders R, Whale AS, Nixon GJ, Cowen S, Ellison SL, et al: An international comparability study on quantification of mRNA gene expression ratios: CCQM-P103.1. Biomol Detect Quantif 2016, 8:15–28
50. Taylor SC, Laperriere G, Germain H: Droplet digital PCR versus qPCR for gene expression analysis with low abundant targets: from variable nonsense to publication quality data. Sci Rep 2017, 7:2409
51. Taylor SC, Carbonneau J, Shelton DN, Boivin G: Optimization of droplet digital PCR from RNA and DNA extracts with direct comparison to RT-qPCR: clinical implications for quantification of Oseltamivir-resistant subpopulations. J Virol Methods 2015, 224: 58–66
52. Jacot D, Greub G, Jaton K, Opota O: Viral load of SARS-CoV-2 across patients and compared to other respiratory viruses. Microbes Infect 2020, 22:617–621
53. Pan Y, Zhang D, Yang P, Poon LLM, Wang Q: Viral load of SARS-CoV-2 in clinical samples. Lancet Infect Dis 2020, 20:411–412
54. Zou L, Ruan F, Huang M, Liang L, Huang H, Hong Z, Yu J, Kang M, Song Y, Xia J, Guo Q, Song T, He J, Yen HL, Peiris M, Wu J: SARS-CoV-2 viral load in upper respiratory specimens of infected patients. N Engl J Med 2020, 382:1177–1179
55. Huang Y, Chen S, Yang Z, Guan W, Liu D, Lin Z, Zhang Y, Xu Z, Liu X, Li Y: SARS-CoV-2 viral load in clinical samples from critically ill patients. Am J Respir Crit Care Med 2020, 201: 1435–1438